7736 *Macromolecules* **2009**, *42*, 7736–7744
DOI: 10.1021/ma901355u

Macromolecules
ARTICLE

An Investigation of Free-Radical Copolymerization Propagation Kinetics of Styrene and 2-Hydroxyethyl Methacrylate

Kun Liang,[†] Marco Dossi,[‡] Davide Moscatelli,[‡] and Robin A. Hutchinson*,[†]

[†]*Department of Chemical Engineering, Dupuis Hall, Queen's University, Kingston, Ontario K7L 3N6, Canada, and* [‡]*Dipartimento di Chimica, Materiali e Ingegneria Chimica "Giulio Natta", Politecnico di Milano, 20131 Milano, Italy*

Received June 24, 2009; Revised Manuscript Received August 22, 2009

ABSTRACT: Free-radical copolymerization propagation kinetics of styrene (ST) and 2- hydroxyethyl methacrylate (HEMA) have been investigated using pulsed laser polymerization (PLP) combined with size exclusion chromatography (SEC) and proton NMR. Monomer reactivity ratios for bulk ST/HEMA copolymerization are $r_{HEMA} = 0.49$ and $r_{ST} = 0.27$, with no significant variation with temperature found between 50 and 120 °C. The composition-averaged copolymerization propagation rate coefficient, $k_{p,cop}$, is well represented by the implicit penultimate unit effect (IPUE) model. The copolymerization kinetics of HEMA with ST is quite similar to that of glycidyl methacrylate (GMA) with ST. A computational study based on quantum chemistry supports the finding that GMA and HEMA are more reactive toward ST radicals compared to alkyl methacrylates.

Introduction

Acrylic copolymers used as binder resins in solvent-borne automotive coatings are produced at high temperature (usually >120 °C) and low solvent levels via free-radical polymerization in a semibatch process. Good reactor control is required to ensure that the copolymer composition and distribution of reactive functional groups are uniform among the copolymer chains produced over the course of the batch. This uniformity is required, as the functional groups on the low molecular weight (MW) chains react on the surface of the vehicle, cross-linking to form the final high MW coating. Thus, a good understanding of copolymer chain-growth kinetics under these higher-temperature conditions is required. We have focused attention on styrene−(ST−) methacrylate (xMA) copolymers, studying the effect of methacrylate ester group (denoted by x) and temperature on polymer composition and propagation kinetics for copolymers of butyl methacrylate (BMA) and ST,[1] dodecyl methacrylate (DMA) and ST[2] and glycidyl methacrylate (GMA) and ST.[3] Although following a general family behavior, small differences were found in the relative reactivity of GMA to ST compared to alkyl methacrylates BMA and DMA. In this work, we extend the study to the copolymerization of ST with 2-hydroxyethyl methacrylate (HEMA), an important functional monomer used in the coatings industry.

Incorporating HEMA into polymer chains has garnered much attention, especially in the biomedical field,[4] because of the monomer's high polarity. Early work demonstrated that the polarity and hydrophilicity of solvents affect copolymer composition and the copolymerization rate of the ST/HEMA system.[5,6] More recently, Schoonbrood et al.[7] used proton NMR to determine the monomer reactivity ratios of ST and HEMA in bulk polymerization, and Sánchez-Chaves et al.[8] described the cumulative composition as a function of conversion and the monomer conversion as a function of polymerization time in *N,N′*-dimethylformamide (DMF) solution. Buback and Kurz[9] have measured propagation rate coefficients (k_p) for the homopolymerization of HEMA by the pulsed laser polymerization (PLP)/ size exclusion chromatography (SEC) technique, finding that the k_p value for HEMA is higher than alkyl methacrylates by a factor of 2. In this article, we apply the PLP/SEC technique to the study of ST/HEMA propagation kinetics as a function of monomer composition over a range of temperatures. In addition, copolymer composition is determined using proton NMR.

From previous studies on ST with methyl methacrylate (MMA),[10] ST/BMA,[1] ST/DMA,[2] and ST/GMA,[3] it is found that the terminal model adequately describes copolymer composition and that the monomer reactivity ratios do not exhibit an observable temperature dependence. In the terminal model, the radical reactivity depends only on the terminal unit of the growing chain such that the mole fraction of monomer-1 in the copolymer (F_1^{inst}) is a function of monomer mole fractions (f_1 and f_2) and the monomer reactivity ratios:[11]

$$F_1^{inst} = \frac{r_1 f_1^2 + f_1 f_2}{r_1 f_1^2 + 2 f_1 f_2 + r_2 f_2^2} \quad (1)$$

Here $r_1 = k_{p11}/k_{p12}$, $r_2 = k_{p22}/k_{p21}$, and k_{pij} is the propagation rate coefficient for addition of monomer-*j* to radical-*i*. Schoonbrood et al.[7] have reported monomer reactivity ratios for bulk ST/HEMA polymerization at 50 °C. In this work we re-examine the system over a wider temperature range.

Although the terminal model succeeds in describing ST/xMA monomer reactivity ratios, it does not represent the variation in the copolymer-averaged propagation rate coefficient, $k_{p,cop}$, as a function of monomer composition. Merz et al.[12] first developed the penultimate model to describe $k_{p,cop}$:

$$k_{p,cop} = \frac{\overline{r_1} f_1^2 + 2 f_1 f_2 + \overline{r_2} f_2^2}{\left(\frac{\overline{r_1} f_1}{k_{11}}\right) + \left(\frac{\overline{r_2} f_2}{k_{22}}\right)} \quad (2)$$

If the penultimate unit does not affect the selectivity of the radicals, $\overline{r}_1 = r_1$ and $\overline{r}_2 = r_2$; Fukuda et al.[13] named this case

*Corresponding author. E-mail: robin.hutchinson@chee.queensu.ca.

 Published on Web 09/01/2009

the implicit penultimate effect (IPUE) model. In addition, $\overline{k}_{11}$ and $\overline{k}_{22}$ can be expressed as functions of monomer fraction

$$\overline{k_{11}} = \frac{k_{p111}(r_1 f_1 + f_2)}{r_1 f_1 + (f_2/s_1)} \quad \overline{k_{22}} = \frac{k_{p222}(r_2 f_2 + f_1)}{r_2 f_2 + (f_1/s_2)} \tag{3}$$

where k_{p111} and k_{p222} are homopolymerization propagation rate coefficients, and radical reactivity ratios s_1 and s_2 are defined as k_{p211}/k_{p111} and k_{p122}/k_{p222}, respectively. ($k_{p,ijk}$ is the propagation rate coefficient for addition of monomer-k to a growing radical-j with unit-i in the penultimate position.) These values can be estimated by fitting the penultimate model to experimental $k_{p,cop}$ vs monomer composition data, usually measured using the PLP/SEC technique.

One of the first applications of the PLP/SEC technique to copolymerization systems was to demonstrate the failure of the terminal model to represent $k_{p,cop}$ data measured at 25 and 55 °C for copolymerization of ST with MMA[14] and other alkyl methacrylates,[15] with the experimental values lower than those calculated according to the terminal model by as much as a factor of 2. The experimental data were well-fit by the IPUE model, with both s values less than unity. Our work has shown that penultimate unit effects remain important at temperatures above 100 °C for ST/BMA, with $k_{p,cop}$ data measured between 50 and 140 °C well fit using temperature-independent values for s.[1] In addition, penultimate unit effects are also important for copolymerization of ST with the functional monomer GMA.[3] As far as we know, the copolymerization propagation kinetics of ST with HEMA have not been studied using the PLP/SEC technique.

Techniques such as PLP/SEC can provide reliable and accurate information about the kinetics of copolymerization reactions. However, the experimental determination of rate coefficients is time-consuming and costly, especially for the diversity of acrylate and methacrylate monomers used in the coatings and adhesives industries. An alternative is to study the reactions based on quantum mechanics, provided that the corresponding computational effort can be managed. Fischer and Radom[16] have explored, both experimentally and computationally, the influence of radical and monomer structure on alkene addition rates to carbon-centered radicals and Heuts et al. applied computational techniques to estimate Arrhenius parameters for propagation in free radical polymerization of ethylene.[17,18] These pioneering studies have been extended to a range of systems and reactions,[19−21] including application to acrylates and methacrylates[22−24] and their copolymerization.[25]

Computational work of Coote et al.,[26] a systematic study of chain length effects for acrylonitrile and vinyl chloride free radical polymerizations, found that rate coefficients largely converged to their long chain limit at the dimer radical stage. Chain length effects were also explored in other studies;[20,23,27−29] generally speaking, the absolute rate coefficients values for the addition of the dimeric or trimeric radical to monomer are closest to experimental data. Fischer and Radom demonstrated, however, that monomeric radical systems provide a good model for predicting and comparing relative rates of monomer addition during polymerization; i.e., copolymerization reactivity ratios.[16] In this work, we simulate the addition reactions of monomeric radicals to monomer, to compare relative rates of methacrylate addition rates to styrene radicals. In particular, we examine whether computational techniques are sensitive enough to capture differences in monomer addition rates found in ST/xMA copolymerization when changing the methacrylate ester group.

Experimental Section

HEMA (97% purity containing 200−220 ppm monomethyl ether hydroquinone), styrene (99% purity, containing 10−15 ppm of 4-*tert*-butylcatechol), photoinitiator DMPA (2,2-dimethoxy-2-phenylacetophenone, 99% purity) and anhydrous DMSO-d_6 (dimethyl sulfoxide-d_6, containing 99.9 atom % D) were all obtained from Sigma-Aldrich and used as received.

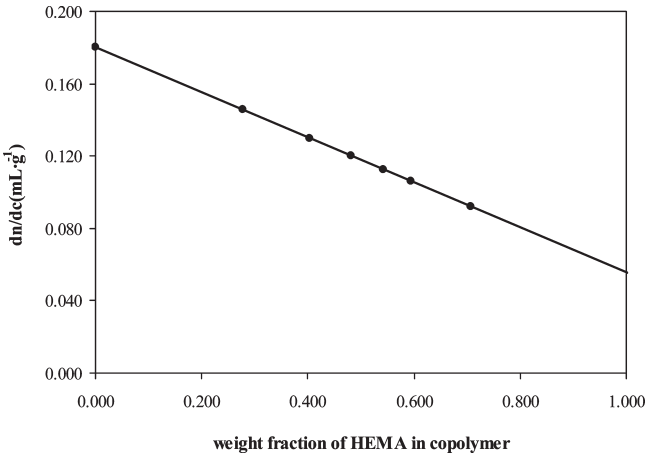

Figure 1. Refractive index (dn/dc) values for styrene/2-hydroxyethyl methacrylate (HEMA) copolymers in THF at 35 °C, plotted as a function of weight fraction HEMA in copolymer.

Low conversion polymerizations were conducted in a pulsed laser setup consisting of a Spectra-Physics Quanta-Ray 100 Hz Nd:YAG laser that is capable of producing a 355 nm laser pulse of duration 7−10 ns and energy of 1−50 mJ per pulse. The laser beam is reflected twice (180°) to shine into a Hellma QS165 0.8 mL jacketed optical sample cell used as the PLP reactor. A digital delay generator (DDG, Stanford Instruments) is attached to the laser in order to regulate the pulse output repetition rate at a value between 10 and 100 Hz. Monomer mixtures in bulk with 5 mmol·L^{-1} DMPA photoinitiator were added to the quartz cell and exposed to laser energy, with temperature controlled by a circulating oil bath. Experiments were run in the temperature range of 50−120 °C, with styrene fraction in the monomer mixture varied between 0 and 100%. Monomer conversions were kept below 5% to avoid significant composition drift, and temperature was controlled to ±1 °C during pulsing.

Polymers produced by PLP were used to determine $k_{p,cop}$ values from analyses of polymer molecular weight distributions (MWD) measured by size exclusion chromatography (SEC). The resulting samples from PLP were precipitated in diethyl ether and the solid polymers were separated from liquid by centrifuge. The polymers were dried in a vacuum oven and then redissolved in THF. Copolymers with greater than 70 mol % HEMA are not THF-soluble, and thus they were not analyzed. Molecular weight distributions were measured with a Waters 2960 separation module connected to a Waters 410 differential refractometer (DRI) and a Wyatt Instruments Dawn EOS 690 nm laser photometer multiangle light scattering (LS) detector. Tethahydrofuran (THF) was used to carry polymers at a flow rate of 1 mL·min^{-1} through the four Styragel columns (HR 0.5, 1, 3, 4) maintained at 35 °C. The DRI detector was calibrated by 10 molecular weight polystyrene standards (870−355 000 Da) with narrow polydispersities, and the LS detector was calibrated by toluene as recommended by the manufacturer.

The refractive index (dn/dc) of the polymer in THF is required to process the data from the LS detector. A Wyatt Optilab DSP refractometer, calibrated with sodium chloride, was used to measure these values for several ST/HEMA copolymer samples. Six samples of 0.1−20 mg·mL^{-1} were prepared in THF for each polymer and injected sequentially to construct a curve with slope dn/dc. As homopolymer of HEMA cannot be dissolved in THF, dn/dc values for ST homopolymer and copolymers of ST/HEMA produced from monomer mixtures containing 0.1−0.7 molar

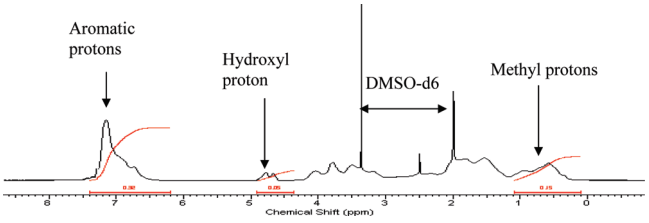

Figure 2. NMR spectrum of copolymer produced at 50 °C from a styrene/2-hydroxyethyl methacrylate (HEMA) monomer mixture containing 30 mol % HEMA.

fractions HEMA were measured as shown in Figure 1, with the homopolymer value for HEMA estimated as 0.0556 $mL \cdot g^{-1}$ by extrapolation.

The polymers isolated from the PLP experiments were also used for composition analysis by proton NMR. The polymer was dissolved in dimethyl sulfoxide for proton NMR analysis conducted at room temperature on a 400 MHz Bruker instrument. The copolymer shows chemical shifts from the aromatic protons in styrene units in the region of 7.4−6.2 ppm and from the methyl protons and hydroxyl protons of main chain HEMA units in the regions 1.1−0.1 ppm and 4.9−4.3 ppm.[7,8] A typical spectrum is shown in Figure 2. Copolymer composition (F_{HEMA} = mol fraction HEMA) was estimated from proton NMR via two methods, either ratioing the area from the ST aromatic protons with the peak area from the HEMA methyl protons

$$F_{\mathrm{HEMA}} = \frac{5A_{H1}}{5A_{H1} + 3A_A} \tag{4}$$

or with the peak area from the hydroxyl proton

$$F_{\mathrm{HEMA}} = \frac{5A_{H2}}{5A_{H2} + A_A} \tag{5}$$

where A_{H1} and A_{H2} are the peak areas of methyl and hydroxyl protons, respectively, and A_A is the peak area of aromatic protons. The polymer compositions estimated by the two methods agreed well with reported values determined using the more distinct hydroxyl peak.

Computational Details. Kinetic parameters were evaluated adopting density functional theory (DFT), which combines good accuracy with a limited computational demand. In particular the Becke 3 parameter and Lee−Yang−Parr functional (B3LYP) were adopted in the DFT calculations to evaluate exchange and correlation energy.[29,30] All quantum chemical calculations of monomeric radical reactants and dimeric radical products were performed with a spin multiplicity of 2 using an unrestricted wave function in order to avoid spin contamination (UB3-LYP). The all electron 6-31 basis set with added polarization functions (6-31G(d6,31,p)) was used for the basis set.

It is generally known that B3LYP methods provide excellent low-cost performance, especially for structure optimizations and frequency calculations.[19,31−34] However recent works[22,23,35] showed that B3LYP is less accurate in the prediction of electronic energies, and new hybrid density functionals have been proposed to study kinetics and reaction mechanisms. In particular Yu at al.[23] pointed out that B3LYP methods lead to activation energies higher than the experimental values, and proposed MPWB1K/6-31*G*(d,p) as an attractive DFT method for obtaining results for acrylate polymerization with quantitative accuracy. The presence of nonsystematic errors in DFT methods was also demonstrated in other studies of radical addition to double bonds.[26,36] These studies all focus on the prediction of absolute rate coefficients. In this work, we show that B3LYP/6-31*G*(d,p) provides estimates for relative rates of monomer addition in good agreement with experiment. In addition, single point calculations were performed with the triple ζ all electron 6-311 basis set with added polarization and diffuse functions (6-311+*G*(d,p))[37] in order to support these findings.

All geometries were fully optimized with the Berny algorithm and were followed by frequency calculations. The geometry of each molecular structure was considered stable only after calculating vibrational frequencies and force constants and if no imaginary vibrational frequency were found. Activation energies and enthalpy changes are determined as

$$E_{\mathrm{a}} = (\mathrm{EE} + \mathrm{ZPE})_{TST} - \sum_{i=reactants} (\mathrm{EE} + \mathrm{ZPE})_i \tag{6}$$

$$\Delta H = \sum_{j=products} (\mathrm{EE} + \mathrm{ZPE} + \mathrm{TC}) - \sum_{i=reactants} (\mathrm{EE} + \mathrm{ZPE} + \mathrm{TC})_i \tag{7}$$

where EE represents the electron energy, ZPE is the zero point energy, and TC is the thermal energy correction. Transition state structures were located adopting the synchronous transit-guided quasi Newton method and were characterized by a single imaginary vibrational frequency.[38] Kinetic constants were determined adopting the conventional transition state theory (TST) as:

$$k(T) = A\mathrm{e}^{-E_a/k_bT} = \frac{k_bT}{h}\frac{q_{\neq}^{rot} q_{\neq}^{vib} q_{\neq}^{el}}{\Pi_{reactants} q^{rot} q^{vib} q^{el}} \mathrm{e}^{-E_a/k_bT} \tag{8}$$

where k_b and h are Boltzmann and Plank constant respectively, T is the temperature, E_a is the activation energy of the process, and $q_{\neq}^{vib}$, $q_{\neq}^{rot}$, q^{vib}, and q^{rot} are the vibrational and rotational partition functions for the transition state and reactants.

One of the main factors that can affect the accuracy of the rate coefficients prediction are the approximations used in calculating the partition functions. In standard *ab initio* calculations the partition functions are constructed using the independent harmonic-oscillator (HO) approximation. However, by analyzing vibrational spectra, and in particular the low vibrational modes of the molecules, it is possible to identify some motions that correspond to internal rotations. These rotations can be free or hindered in relation to the presence of structural features inhibiting the motions.[32,39] The importance of considering the low vibrational frequencies as internal rotations is well documented in the literature, for addition reactions of radicals to olefins especially.[17,18,21,23,25,26,32,39−41] In particular, by taking into account the internal rotation in the transition state, the pre-exponential factor increases and in some case the value is double. However, the activation energy value is unaffected and remains almost constant.[32,39−41]

If the computational accuracy is improved by treating the low frequency torsional modes as internal rotations, it has also been shown that the corrections on the partition functions can be more or less critical in relation to the type of system investigated. In particular the corrections are moderately temperature dependent, but seem to be most pronounced at higher temperatures.[21,41] Moreover the contribution of internal rotations becomes larger as the molecules investigated gets larger[40] and finally the correction for the internal rotation about the addition of the same carbon-centered radical to different unsaturated compounds is close to unity.[21]

In the present work, the addition of styrene radical to different methacrylate monomers was studied at relatively low temperature and, due to the consideration proposed above, the rate coefficients were calculated using standard transition state theory with the partition functions determined under the HO approximation. As the primary goal of this numerical application is to compare the reactivity of ST−xMA systems, the proposed level of theory is sufficient for reasonable estimates of the rate coefficients.[26] All quantum chemistry calculations

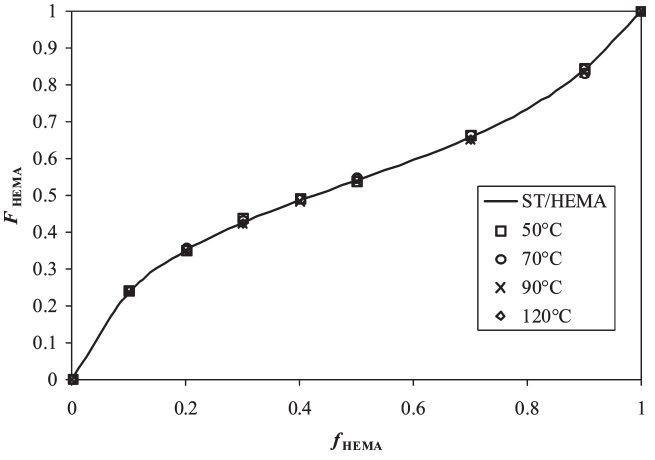

Figure 3. Copolymer composition data for low-conversion styrene/2-hydroxyethyl methacrylate (HEMA) bulk copolymerization at varying temperatures, plotting mole fraction HEMA in copolymer (F_{HEMA}) as a function of HEMA mole fraction in the monomer phase (f_{HEMA}). The solid curve is the prediction of the terminal copolymerization model with literature[7] monomer reactivity ratios $r_{HEMA} = 0.49$ and $r_{ST} = 0.27$.

were performed with the Gaussian 03 suite of programs and all pictures drawn with Molden 4.2.[42,43]

Results and Discussion

An important assumption of both the terminal and penultimate models is that the monomer addition reactions are irreversible. For methacrylate systems, depropagation can occur at appreciable rates at higher temperatures (> 120 °C), depending on monomer concentrations.[44,45] However, our previous work[1,3] has shown that depropagation does not affect low conversion bulk ST/xMA copolymerization at temperatures below 130 °C; thus depropagation does not need to be considered for this study.

Monomer Reactivity Ratios. As only a single ST/HEMA bulk copolymerization study was found in literature, it is necessary to verify the monomer reactivity ratios reported for 50 °C. In addition, it is important to examine whether the values vary with temperature. Low conversion PLP experiments were carried out from 50 to 120 °C and the resulting polymer compositions were analyzed by NMR. The full set of experimental conditions and results is summarized in Table S1, with a plot of HEMA mole fraction in the copolymer plotted against monomer composition in Figure 3. The copolymer composition curve has the shape commonly observed for ST-xMA systems, and the data are well-represented by the Mayo−Lewis terminal model using the literature monomer reactivity ratios of $r_{HEMA} = 0.49$ and $r_{ST} = 0.27$.[7] In addition, the data indicate that there is no significant effect of temperature on copolymer composition, with data up to 120 °C well represented by the same set of r values.

It is interesting to compare these results to other ST/xMA systems. Table 1 summarizes monomer reactivity ratios for ST copolymerized with MMA, BMA, DMA, GMA and HEMA, and Figure 4 presents the corresponding Mayo−Lewis curves for these systems. The curves for ST/HEMA and ST/GMA are very similar, and differ significantly from the curves for the three alkyl methacrylates. With GMA and HEMA, methacrylate-enriched copolymer is produced in styrene-rich monomer mixtures relative to the alkyl methacrylates, a difference captured by the lower r_{ST} value. A computational study has been done to explore these reactivity differences, as presented later.

Copolymerization Propagation Kinetics. The PLP/SEC technique has proven to be an efficient and accurate method

Table 1. Monomer Reactivity Ratios for Copolymerization of Styrene (ST) with Various Methacrylates[a]

	ST/HEMA[7]	ST/GMA[3]	ST/BMA[1]	ST/DMA[2]	ST/MMA[10]
r_{ST}	0.27	0.31	0.61	0.57	0.49
r_{xMA}	0.49	0.51	0.42	0.45	0.49

[a] 2-Hydroxyethyl methacrylate (HEMA), glycidyl methacrylate (GMA), butyl methacrylate (BMA), dodecyl methacrylate (DMA), and methyl methacrylate (MMA).

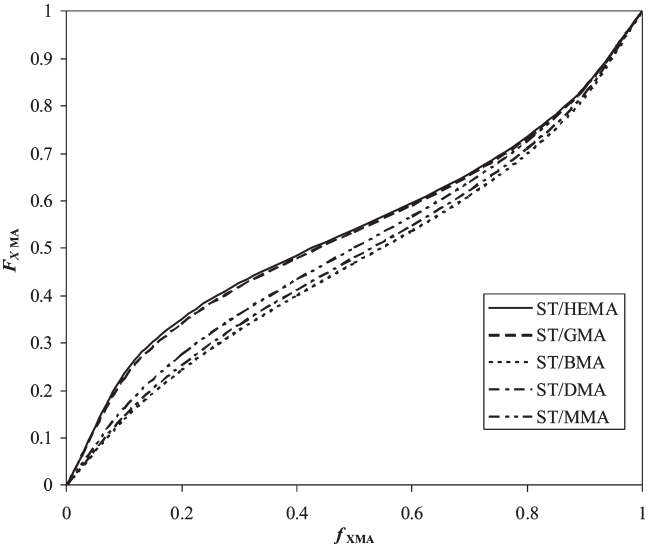

Figure 4. Mole fraction methacrylate in copolymer (F_{xMA}) vs mole fraction in monomer mixture (f_{xMA}) for ST/HEMA, ST/GMA, ST/BMA, ST/DMA, and ST/MMA, calculated using the monomer reactivity ratios in Table 1.

to investigate $k_{p,cop}$, based on careful analysis of polymer MWDs. In PLP experiments, each laser flash initiates new radicals from photoinitiator, with these radicals propagating and, in some cases, terminating in the time period between two flashes. Those radicals that survive the dark period between pulses are likely to be terminated by the next laser flash, forming a significant population of dead chains with length L_0

$$L_0 = k_{p,cop}[M]t_0 \quad (9)$$

Given the total monomer concentration [M] and flash interval t_0, the copolymer-averaged propagation rate coefficient $k_{p,cop}$ can be deduced. There is a probability that some radicals survive the next laser flash and terminate with a later flash, such that signals corresponding to chains of length $2L_0$ and $3L_0$, can also be observed. If well-structured MWDs are formed, like those shown in Figure 5, $k_{p,cop}$ values can be calculated from the first inflection point of the MWD according to

$$k_{p,cop}/L\cdot mol^{-1}s^{-1} = \frac{MW_0}{1000\rho t_0} \quad (10)$$

where MW_0 is the polymer molecular weight at the first inflection point and ρ ($g\cdot mL^{-1}$) is the density of monomer mixture calculated assuming volume additivity. In addition, the MW value at the second inflection point should occur at a value of twice that of MW_0, providing an important check for PLP consistency.

The parameters necessary to estimate $k_{p,cop}$ from SEC data are summarized in Table 2, with monomer densities calculated as a function of temperature, and the refractive

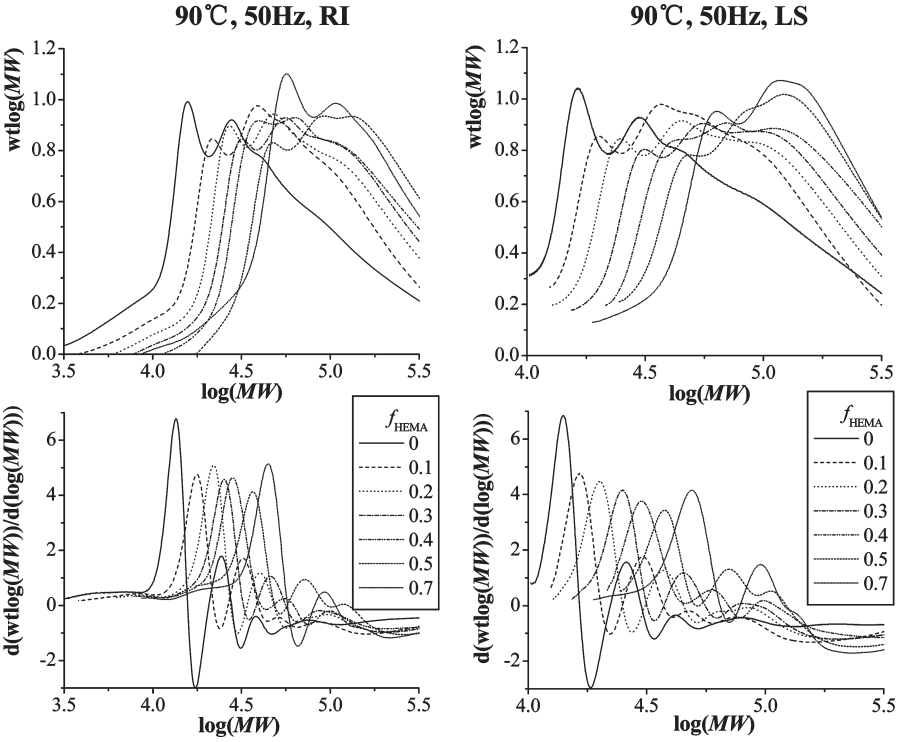

Figure 5. MWDs (top) and corresponding first derivative (bottom) plots obtained for styrene/2-hydroxyethyl methacrylate (HEMA) copolymer produced by PLP at 90 °C and 50 Hz, as measured by RI (left) and LS (right) detectors. Monomer compositions are given as mole fraction HEMA (f_{HEMA}).

Table 2. Parameters for Calculation of $k_{p,cop}$ from SEC Analysis of PLP-Generated Copolymer Samples of Styrene with 2-Hydroxyethyl Methacrylate (HEMA)

			Mark−Houwink parameters	
monomer	density ρ (g·mL^{-1})	dn/dc (mL·g^{-1})	K (dL·g^{-1}) × 10^{-4}	a
styrene	$0.9193 - 0.000\,665T$/°C[46]	0.180[1]	1.14[1]	0.716[1]
HEMA	$1.092 - 0.000\,98T$/°C[9]	0.0556	2.39	0.537

index (dn/dc) for interpretation of LS results measured as discussed previously. However, Mark−Houwink parameters for HEMA homopolymer are required in order to analyze the output from the RI detector, with the copolymer MW calculated as a composition-weighted average of the homopolymer values, as done previously.[1,3,10] As the homopolymer of HEMA cannot be dissolved in THF, these values have been estimated. The "a" exponent value was set to the value reported for GMA,[3] and the "K" was adjusted to achieve agreement between LS and RI MW results for ST/HEMA produced with $f_{HEMA} \leq 0.7$, according to the following relations:

$$\log(\mathrm{MW})_{\mathrm{HEMA}} = \frac{1 + a_{\mathrm{S}}}{1 + a_{\mathrm{HEMA}}} \log(\mathrm{MW})_{\mathrm{S}} + \frac{1}{1 + a_{\mathrm{HEMA}}} \log\left(\frac{K_{\mathrm{S}}}{K_{\mathrm{HEMA}}}\right) \quad (11)$$

$$\log(\mathrm{MW})_{\mathrm{cop}} = (1 - w_{\mathrm{HEMA}}) \log(\mathrm{MW})_{\mathrm{S}} + w_{\mathrm{HEMA}} \log(\mathrm{MW})_{\mathrm{HEMA}} \quad (12)$$

Here, w_{HEMA} is the weight fraction of HEMA in the copolymer. This methodology to establish calibration for the RI detector is not ideal, as it depends upon the accuracy of the LS results. However, as the LS results are processed using experimentally determined dn/dc values for the copolymers, the RI results are used only as a check on SEC operation. Agreement between the two detectors was good, within 10%, over a wide range of MW_0 values, between 5×10^3 and 1×10^5 Da.

A systematic PLP/SEC study with experiments from 50 to 120 °C has been carried out, with complete experimental conditions and results summarized in Table S1. Most experiments were conducted at 50 Hz; a few experiments were run with a pulse repetition rate of 33 Hz, with the $k_{p,cop}$ values obtained in good agreement with 50 Hz results. Above 120 °C, no meaningful PLP structure was obtained, possibly due to styrene thermal polymerization and/or cross-linking involving HEMA impurities. Typical results are shown in Figure 5, a plot of copolymer MWDs measured by the two detectors for comonomer mixtures of varying composition pulsed at 90 °C with a laser repetition rate of 50 Hz, and the corresponding first-derivative plots used to identify inflection points. The MWDs shift to the right and the corresponding MW_0 values increase as the mole fraction of HEMA in the comonomer mixture increases from 0 to 0.7. This shift is not surprising, as the propagation rate coefficient for HEMA is seven times greater than that of ST at 90 °C, as calculated according to the Arrhenius equations determined from previous PLP/SEC studies:[9,46]

$$k_{\mathrm{p,ST}}/\mathrm{L \cdot mol^{-1} \cdot s^{-1}} = 10^{7.630} \exp(-3910/(T/\mathrm{K})) \quad (13)$$

$$k_{\mathrm{p,HEMA}}/\mathrm{L \cdot mol^{-1} \cdot s^{-1}} = 10^{6.954} \exp(-2634/(T/\mathrm{K})) \quad (14)$$

The $k_{p,cop}$ data obtained at 50 °C is plotted in Figure 6 as a function of monomer composition. The value increases from

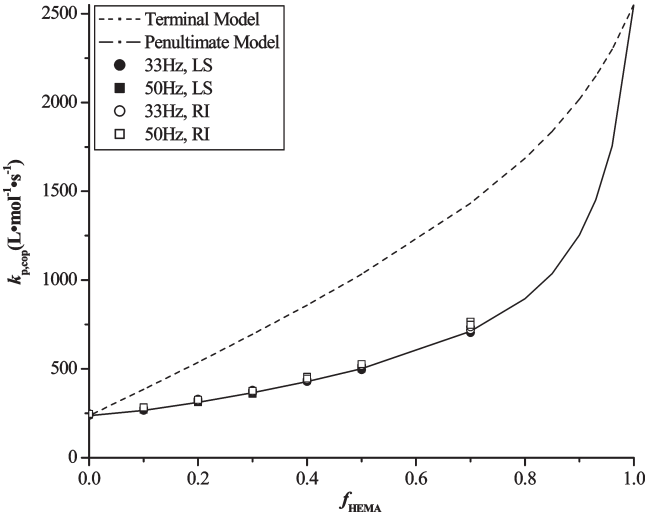

Figure 6. Copolymer propagation rate coefficients ($k_{p,cop}$) data vs 2-hydroxyethyl methacrylate (HEMA) monomer mole fraction, as measured by PLP/SEC at 50 °C. Terminal model predictions are indicated by dashed line and penultimate model fit, calculated with $s_{ST} = 0.38$ and $s_{HEMA} = 1.34$, by the solid line.

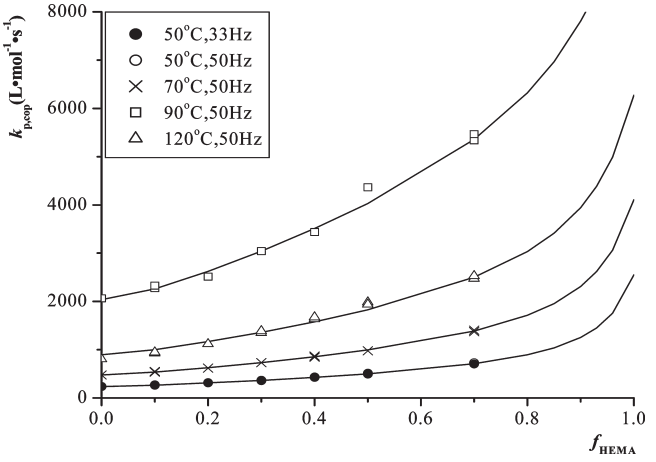

Figure 7. Experimental $k_{p,cop}$ (L·mol^{-1}·s^{-1}) values determined by SEC analysis of styrene/2-hydroxyethyl methacrylate (HEMA) copolymers produced via PLP experiments, plotted as a function of HEMA monomer mole fraction. Lines indicate data fits using the implicit penultimate unit effect model, with $s_{ST} = 0.38$ and $s_{HEMA} = 1.34$.

the ST homopolymer value of 240 to 700 L·mol^{-1}·s^{-1} with $f_{HEMA} = 0.7$. As mentioned before, the agreement between the $k_{p,cop}$ estimated from LS and RI detectors is excellent, as is the agreement between experiments run at 33 and 50 Hz. Also shown in Figure 6 is the prediction of the terminal model, calculated using the monomer reactivity ratios that describe the copolymer composition data, $r_{HEMA} = 0.49$ and $r_{ST} = 0.27$, and the homopolymer k_p values calculated according to eq 13 and 14. The deviation between experiment and the terminal model prediction is significant, with the terminal model overpredicting $k_{p,cop}$ by as much as a factor of 2. It is clear that the terminal model cannot simultaneously describe copolymer composition and reaction rate for the ST/HEMA system, as observed previously for ST copolymerized with alkyl methacrylates[1,10,14,15] and with the functional monomer GMA.[3] As for these other systems, the IPUE model provides a good fit to the experimental data with a ST radical reactivity ratio of less than unity. Radical reactivity ratios were estimated using the nonlinear parameter estimation capabilities of the computer package Predici[47] by fitting of eqs 2 and 3 to the experimental $k_{p,cop}$ data in the entire 50−120 °C temperature range as a function of f_{HEMA}, with equal weighting on all data points and monomer reactivity ratios and $k_{p,iii}$ values set according to previous literature. The package uses a Gauss−Newton technique, estimating 95% confidence intervals from the variance-covariance matrix.[48] The values $s_{ST} = 0.38 \pm 0.01$ and $s_{HEMA} = 1.34 \pm 0.71$, estimated by nonlinear regression, are able to fit the entire set of $k_{p,cop}$ data between 50 and 120 °C, as determined by LS analysis and shown in Figure 7. The much higher uncertainty in the s_{HEMA} estimate is due to the lack of $k_{p,cop}$ data for HEMA-rich mixtures ($f_{HEMA} > 0.7$). While enthalpic contributions cannot be ruled out, a single pair of temperature-independent s values is sufficient to represent the data, as found previously for the ST/BMA[1] and ST/GMA[3] systems.

Table 3 summarizes the kinetic coefficients for these three ST methacrylate systems. (The reactivity ratios of ST/MMA and ST/DMA are very similar to ST/BMA.) It is difficult to determine whether the difference in the s values reflects real kinetic differences, or is a reflection of the higher uncertainty in estimating these coefficients.[10] Despite the difference in absolute k_p values for the three methacrylates, the relative addition of styrene to methacrylate radicals is similar (r_{xMA} between 0.4 and 0.5). However, the functional monomers GMA and HEMA add onto a styrene radical significantly faster than does BMA, as reflected in the lower r_{ST} values.

Table 3. Comparison of Reactivity Ratios for Copolymerization of Styrene (ST) with 2-Hydroxyethyl (HEMA), Glycidyl (GMA), and Butyl (BMA) Methacrylates

	ST/HEMA	ST/GMA[3]	ST/BMA[1]
r_{ST}	0.27	0.31	0.61
r_{xMA}	0.49	0.51	0.42
s_{ST}	0.38	0.28	0.44
s_{xMA}	1.34	1.05	0.62
$k_{p,xMA}$[a]	4108[9]	1638	1233

[a] In L·mol^{-1}·s^{-1} calculated at 70 °C.

Computational Study of ST/xMA Reactivity. A computational study was done to explore the reactivity between ST and various methacrylates. As a preliminary study, the Arrhenius propagation and depropagation parameters for ST, HEMA, GMA, BMA, and MMA were calculated at 100 °C as discussed in the Computational Details and compared with the experimental data reported in literature, as summarized in Table 4. There is good agreement between experimental and computational values, in particular for the propagation and depropagation activation energies. The discrepancy between computational and experimental values is ~1 kcal·mol^{-1}, comparable with experimental uncertainty. The prediction of the pre-exponential factor (A) is less accurate. As discussed in the Introduction, some of the differences may arise as the computation examines monomer addition to a monomeric, rather than a long-chain, radical. Moreover, another source of inaccuracy is the use of the HO approximation, as well presented in the Computational Details. However, these effects should not influence the study of the relative reactivity of styrene toward the methacrylates, as will be shown.

For the computational determination of the monomer reactivity ratios at a given temperature, the pre-exponential factors for the copolymerization kinetic coefficients are considered to be equal to the corresponding values for the homopolymerization reactions. In particular the pre-exponential factor for methacrylate monomer addition to styrene radical ($A_{ST,xMA}$) is set equal to the pre-exponential

Table 4. Comparison between Arrhenius Propagation and Depropagation Parameters for ST, HEMA, GMA, BMA, and MMA, both Theoretically and Experimentally Determined[a]

	(computational)			(experimental)			(computational)		(experimental)	
monomer	$\ln(A_p)$	E_p	k_p* (100 °C)	$\ln(A_p)$	E_p	k_p (100 °C)	$\ln(A_{dep})$	E_{dep}	$\ln(A_{dep})$	E_{dep}
ST[46]	18.99	8.28	2.49×10^3	17.57	7.77	1.20×10^3	30.12	22.36		
HEMA[9]	16.34	6.39	2.47×10^3	16.00	5.23	7.66×10^3	30.25	18.90		
GMA[3]	17.15	6.58	3.93×10^3	15.44	5.47	3.16×10^3	30.04	18.32	30.18	18.33
BMA[49,50]	17.42	6.34	7.08×10^3	15.15	5.47	2.37×10^3	29.85	19.09	29.53	17.87
MMA[51]	16.35	6.21	2.90×10^3	14.80	5.34	1.99×10^3	30.71	18.90		

[a] Key: styrene (ST), 2-hydroxyethyl methacrylate (HEMA), glycidyl methacrylate (GMA), butyl methacrylate (BMA), methyl methacrylate (MMA). References are for experimental results. Activation energies (E_p, E_{dep}) in kcal·mol^{-1}, A_p in L·mol^{-1}·s^{-1}, and A_{dep} in s^{-1}, k_p in L·mol^{-1}·s^{-1}. The notation k_p* indicates that the computation examines monomer addition to a monomeric radical.

Table 5. Comparison between Computational and Experimental Monomer Reactivity Ratios for Addition to a Styrene Radical in Styrene/Methacrylate Copolymerizations.[a]

Data	ST/ST	ST/HEMA	ST/GMA	ST/BMA	ST/MMA
$\ln(A_p)$ (computational)	18.99	18.99	18.99	18.99	18.99
E_p (computational)	8.28	7.09	7.47	7.71	7.75
k_p* (computational)	2.49×10^3	12.37×10^3	7.37×10^3	5.39×10^3	5.05×10^3
r_{ST} (computational)	–	0.20	0.34	0.46	0.49
r_{ST} (experimental)	–	0.27	0.31	0.61	0.49

[a] Key: styrene (ST), 2-hydroxyethyl methacrylate (HEMA), glycidyl methacrylate (GMA), butyl methacrylate (BMA), and methyl methacrylate (MMA). Computational energies reported in kcal·mol^{-1}, pre-exponential factors and kinetic coefficients (calculated at 100 °C) in L·mol^{-1}·s^{-1}. The notation k_p* indicates that the computation examines monomer addition to a monomeric radical.

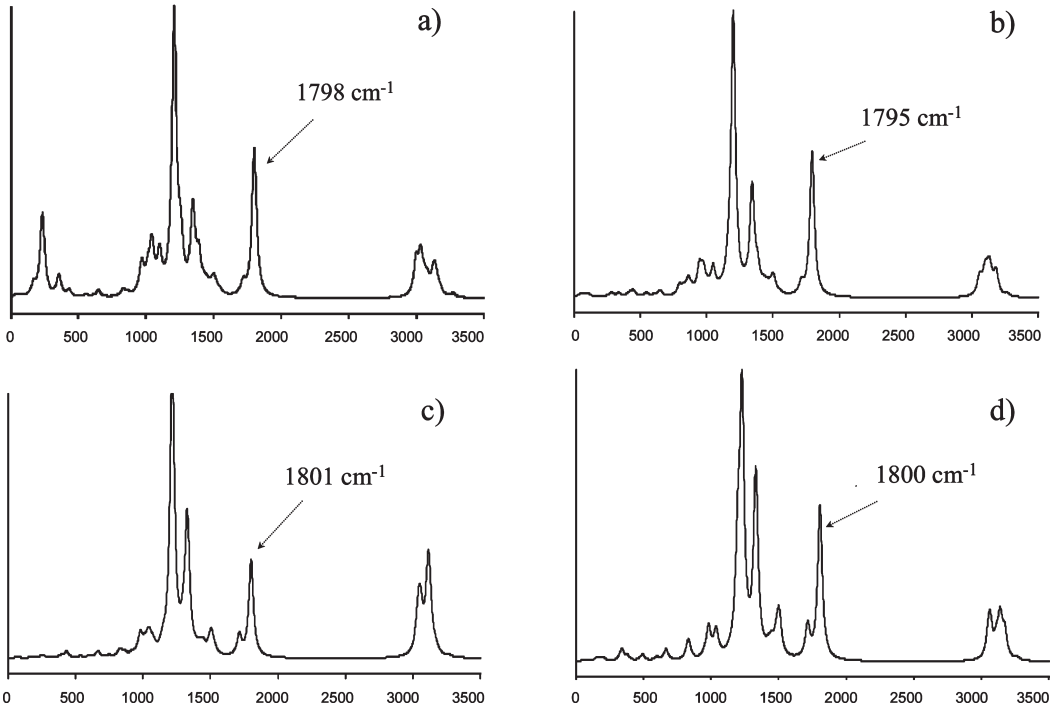

Figure 8. Simulated IR spectra: (a) 2-hydroxyethyl methacrylate, (b) glycidyl methacrylate, (c) butyl methacrylate, and (d) methyl methacrylate.

factor for styrene homopolymerization ($A_{ST,ST}$). According to this hypothesis, the pre-exponential factor is a function of the radical involved and thus is assumed to be fully independent of the monomer reacting. This hypothesis agrees with findings and assumptions proposed by Fischer and Radom[16] and removes the uncertainty related to the evaluation of the pre-exponential factors.

Taking these considerations into account, the copolymerization reactions of ST with HEMA, GMA, BMA and MMA were simulated at 100 °C with B3LYP/6-31*G*(d,p) to study the differences in the reactivity of various methacrylates with styrene, specifically the value of r_{ST}. The kinetic parameters for all these reactions are summarized in Table 5. From these data it is possible to calculate the corresponding values of r_{ST} and compare to experimental results. Complete information regarding optimized molecular structures of reactants, products and transition states involved in the reactions is available as Table S2 in the Supporting Information.

Data reported in Table 5 show good agreement between experimental values from PLP/SEC studies and computational values obtained adopting quantum chemistry calculations. Moreover this computational study confirms that the ST radical is more reactive toward HEMA and GMA than other alkyl methacrylates. The effect of temperature on the monomer reactivity ratio values was also considered. The computational results predict a slight increase in r_{ST} values of 0.07 or less for all systems as temperature is increased from

50 to 120 °C; e.g., r_{ST} increases from 0.29 to 0.36 for the ST/GMA system. This increase is larger than the standard deviation reported for the ST/BMA[1] (±0.03) and ST/GMA[3] ((±0.01−0.06, depending on temperature) experimental studies. However, a detailed analysis of the ST/GMA data found that r_{ST} increased slightly from 0.29 to 0.34 between 50 and 150 °C.[3] Computational studies may prove to be a more sensitive probe of this behavior than experiment.

As discussed in the Computational Details, single point calculations were performed with the larger basis set 6-311+G(d,p)[37] in order to support the results obtained with the B3LYP/6-31G(d,p) level of theory. It was found that the monomer reactivity ratios calculated are only slightly influenced by the basis set size. In particular r_{ST} is calculated to be 0.25 for ST/HEMA, 0.42 for ST/GMA, 0.54 for ST/BMA and 0.52 for ST/MMA. The increases in r_{ST} values are 0.04 or less for all systems as temperature is increased from 50 to 120 °C. These results indicate that the smaller basis set provides sufficient accuracy when examining relative rates of addition to the ST radical.

Previously, it was noted that the difference in reactivity with methacrylate type is correlated to a shift in the methacrylate carbonyl IR peak.[3,52] Thus, IR spectra of the monomers were plotted from the quantum mechanics simulations, as shown in Figure 8, with the frequencies of the carbonyl group for each monomer indicated. The carbonyl IR peaks for HEMA and GMA are shifted to a lower wavelength relative to BMA or MMA. In particular the carbonyl IR peak for HEMA is shifted by 3 and 2 cm^{-1} respectively, whereas the peak for GMA is shifted to a lower value by 6 and 5 cm^{-1}. The reason behind this correlation between relative reactivity and the shift in carbonyl peak position is not known, and it should be further explored.

Conclusions

The PLP technique has been employed to systematically investigate free radical bulk copolymerization of ST and HEMA in the temperature range 50−120 °C. SEC analysis of the polymer MWDs produced by PLP was possible in THF solvent only for copolymers produced from monomer mixtures with HEMA mole fraction of 0.7 or lower. Nonetheless, a refractive index (dn/dc) of pHEMA could be extrapolated by measuring values for the THF-soluble copolymers. The composition-averaged copolymer propagation rate coefficients ($k_{p,cop}$) are well-described by the implicit penultimate unit effect (IPUE) model.

Copolymer composition data, determined via proton NMR, are well-represented by the terminal model using monomer reactivity ratios taken from literature, with no significant temperature dependence observed. HEMA, as found previously for GMA, exhibits higher reactivity to ST radicals than do alkyl methacrylates such as MMA, BMA, and DMA. The same behavior, also found in a computational study, may be correlated to shifts in the IR carbonyl peak. Further studies to explore this relationship are underway.

Acknowledgment. We thank E. I. du Pont de Nemours and Co. and the Natural Sciences and Engineering Research Council of Canada for financial support of this work, and Prof. Dr. Sabine Beuermann of Potsdam University for helpful discussions.

Supporting Information Available: Table S1, summarizing detailed PLP/SEC and NMR results for ST/HEMA copolymerization, and Table S2, collecting all of the optimized molecular geometries used in the computational determination of monomer reactivity ratios. This material is available free of charge via the Internet at http://pubs.acs.org.

References and Notes

(1) Li, D.; Li, N.; Hutchinson, R. A. *Macromolecules* **2006**, *39*, 4366–4373.
(2) Wang, W.; Hutchinson, R. A. *Macromol. React. Eng.* **2008**, *2*, 199–214.
(3) Wang, W.; Hutchinson, R. A. *Macromolecules* **2008**, *41*, 9011–9018.
(4) Wichterle. *Encyclopedia of Polymer Technology*: Wiley: New York, 1971; *Vol. 15*, pp 275−281.
(5) Okano, T.; Aoyagi, J.; Shinohara, J. *Nippon Kagaku Kaishi.* **1976**, *1*, 161–175.
(6) Lebduška, J.; Šnupárek, J., Jr.; Kašpar, K.; Čermák, V. *J. Polym. Sci., Part A: Polym. Chem.* **1986**, *24*, 777–791.
(7) Schoonbrood, H. A. S.; Aerdts, A. M.; German, A. L.; van der Velden, G. P. M. *Macromolecules* **1995**, *28*, 5518–5525.
(8) Sánchez-Chaves, M.; Martinez, G.; Madruga, E. L. *J. Polym. Sci., Part A: Polym. Chem.* **1999**, *37*, 2941–2948.
(9) Buback, M.; Kurz, C. *Macromol. Chem. Phys.* **1998**, *199*, 2301–2310.
(10) Coote, M. L.; Zammit, M. D.; Davis, T. P.; Willett, G. D. *Macromolecules* **1997**, *30*, 8191–8204.
(11) Mayo, F. R.; Lewis, F. M. *J. Am. Chem. Soc.* **1944**, *66*, 1594–1601.
(12) Merz, E.; Alfrey, T.; Goldfinger, G. *J. Polym. Sci.* **1946**, *1*, 75–82.
(13) Fukuda, T.; Ma, Y.; Inagaki, H. *Macromolecules* **1985**, *18*, 26–31.
(14) Davis, T. P.; O'Driscoll, K. F.; Piton, M. C.; Winnik, M. A. *J. Polym. Sci., Part C: Polym. Lett.* **1989**, *27*, 181–185.
(15) Davis, T. P.; O'Driscoll, K. F.; Piton, M. C.; Winnik, M. A. *Macromolecules* **1990**, *23*, 2113–2119.
(16) Fischer, H.; Radom, L. *Angew. Chem., Int. Ed.* **2001**, *40*, 1340–1371.
(17) Heuts, J. P. A.; Gilbert, R. G.; Radom, L. *Macromolecules* **1995**, *28*, 8771–8781.
(18) Heuts, J. P. A.; Gilbert, R. G.; Radom, L. *J. Phys. Chem.* **1996**, *100*, 18997–19006.
(19) Van Speybroeck, V.; Van Cauter, K.; Coussens, B.; Waroquier, M. *ChemPhysChem* **2005**, *6*, 180–189.
(20) Van Cauter, K.; Van Speybroeck, V.; Vansteenkiste, P.; Reyniers, M. F.; Waroquier, M. *ChemPhysChem* **2006**, *7*, 131–140.
(21) Sabbe, M. K.; Reyniers, M. F.; Van Speybroeck, V.; Waroquier, M.; Marin, G. B. *ChemPhysChem* **2008**, *9*, 124–140.
(22) Degirmeci, I.; Avci, D.; Aviyente, V.; Van Cauter, K.; Van Speybroeck, V.; Waroquier, M. *Macromolecules* **2007**, *40*, 9599–9602.
(23) Yu, X.; Pfaendtner, J.; Broadbelt, L. J. *J. Phys. Chem. A* **2008**, *112*, 6772–6782.
(24) Degirmeci, I.; Aviyente, V.; Van Speybroeck, V.; Waroquier, M. *Macromolecules* **2009**, *42*, 3033–3041.
(25) Yu, X.; Levine, S. E.; Broadbelt, L. J. *Macromolecules* **2008**, *41*, 8242–8251.
(26) Izgorodina, E. I.; Coote, M. L. *Chem. Phys.* **2006**, *324*, 96–110.
(27) Moscatelli, D.; Dossi, M.; Cavallotti, C.; Storti, G. *Macromol. Symp.* **2007**, *259*, 337–347.
(28) Van Cauter, K.; Van den Bossche, B. J.; Van Speybroeck, V.; Waroquier, M. *Macromolecules* **2007**, *40*, 1321–1331.
(29) Becke, A. D. *J. Chem. Phys.* **1993**, *98*, 5648–5652.
(30) Lee, C.; Yang, W.; Parr, R. G. *Phys. Rev. B* **1988**, *37*, 785–789.
(31) Wong, M. W.; Radom, L. *J. Phys. Chem. A* **1998**, *102*, 2237–2245.
(32) Van Speybroeck, V.; Van Neck, D.; Waroquier, M.; Wauters, S.; Saeys, M.; Marin, G. B. *J. Phys. Chem. A* **2000**, *104*, 10939–10950.
(33) Gomez-Balderas, R.; Coote, M. L.; Henry, D. J.; Radom, L. *J. Phys. Chem. A* **2004**, *108*, 2874–2883.
(34) Coote, M. L. *J. Phys. Chem. A* **2004**, *108*, 3865–3872.
(35) Hemelsoet, K.; Moran, D.; Van Speybroeck, V.; Waroquier, M.; Radom, L. *J. Phys. Chem. A* **2006**, *110*, 8942–8951.
(36) Izgorodina, E. I.; Coote, M. L.; Radom, L. *J. Phys. Chem. A* **2005**, *109*, 7558–7566.
(37) Dunning, T. H.; Hay, P. J. In *Modern Theoretical Chemistry*; Schaefer, H. F., Ed.; Plenum: New York, 1976; p 1.
(38) Peng, C.; Ayala, P. Y.; Schlegel, H. B.; Frisch, M. J. *J. Comput. Chem.* **1996**, *17*, 49–56.
(39) Van Speybroeck, V.; Van Neck, D.; Waroquier, M. *J. Phys. Chem. A* **2002**, *106*, 8945–8950.
(40) Vansteenkiste, P.; Van Speybroeck, V.; Marin, G. B.; Waroquier, M. *J. Phys. Chem. A* **2003**, *107*, 3139–3145.

(41) Vansteenkiste, P.; Van Neck, V.; Van Speybroeck, V.; Waroquier, M. *J. Chem. Phys.* **2006**, *124*, Art. No. 044314.
(42) Frisch, M. J.; Trucks, G. W.; Schlegel, H. B.; Scuseria, G. E.; Robb, M. A.; Cheeseman, J. R.; Montgomery, J. A., Jr.; Vreven, T.; Kudin, K. N.; Burant, J. C.; Millam, J. M.; Iyengar, S. S.; Tomasi, J.; Barone, V.; Mennucci, B.; Cossi, M.; Scalmani, G.; Rega, N.; Petersson, G. A.; Nakatsuji, H.; Hada, M.; Ehara, M.; Toyota, K.; Fukuda, R.; Hasegawa, J.; Ishida, M.; Nakajima, T.; Honda, Y.; Kitao, O.; Nakai, H.; Klene, M.; Li, X.; Knox, J. E.; Hratchian, H. P.; Cross, J. B.; Bakken, V.; Adamo, C.; Jaramillo, J.; Gomperts, R.; Stratmann, R. E.; Yazyev, O.; Austin, A. J.; Cammi, R.; Pomelli, C.; Ochterski, J. W.; Ayala, P. Y.; Morokuma, K.; Voth, G. A.; Salvador, P.; Dannenberg, J. J.; Zakrzewski, V. G.; Dapprich, S.; Daniels, A. D.; Strain, M. C.; Farkas, O.; Malick, D. K.; Rabuck, A. D.; Raghavachari, K.; Foresman, J. B.; Ortiz, J. V.; Cui, Q.; Baboul, A. G.; Clifford, S.; Cioslowski, J.; Stefanov, B. B.; Liu, G.; Liashenko, A.; Piskorz, P.; Komaromi, I.; Martin, R. L.; Fox, D. J.; Keith, T.; Al-Laham, M. A.; Peng, C. Y.; Nanayakkara, A.; Challacombe, M.; Gill, P. M. W.; Johnson, B.; Chen, W.; Wong, M. W.; Gonzalez, C.; Pople, J. A. *Gaussian 03, revision C.02*; Gaussian, Inc.: Wallingford, CT, 2004.
(43) Schaftenaar, G.; Noordik, J. H. *J. Comput.-Aided Mol. Design* **2000**, *14*, 123–134.
(44) Bywater, S. *Trans. Faraday Soc.* **1955**, *51*, 1267–1273.
(45) Hutchinson, R. A.; Paquet, D. A., Jr.; Beuermann, S.; McMinn, J. H. *Ind. Eng. Chem. Res.* **1998**, *37*, 3567–3574.
(46) Buback, M.; Gilbert, R. G.; Hutchinson, R. A.; Klumperman, B.; Kuchta, F.; Manders, B. G.; O'Driscoll, K. F.; Russell, G. T.; Schweer, J. *Macromol. Chem. Phys.* **1995**, *196*, 3267–3280.
(47) Wulkow, M. *Macromol. React. Eng.* **2008**, *2*, 461–494.
(48) Wulkow, M. *Predici 6.37.8*; Computing in Technology GmbH: Rastede, Germany 2003.
(49) Beuermann, S.; Buback, M.; Davis, T. P.; Gilbert, R. G.; Hutchinson, R. A.; Kajiwara, A.; Klumperman, B.; Russell, G. T. *Macromol. Chem. Phys.* **2000**, *201*, 1355–1364.
(50) Wang, W.; Hutchinson, R. A.; Grady, M. C. *Ind. Eng. Chem. Res.* **2009**, *48*, 4810–4816.
(51) Beuermann, S.; Buback, M.; Davis, T. P.; Gilbert, R. G.; Hutchinson, R. A.; Olaj, O. F.; Russell, G. T.; Schweer, J.; van Herk, A. M. *Macromol. Chem. Phys.* **1997**, *198*, 1545–1560.
(52) Woecht, I.; Schmidt-Naake, G.; Beuermann, S.; Buback, M.; Garcia, N. *J. Polym. Sci., Part A: Polym. Chem.* **2008**, *46*, 1460–1469.